FISCHER-TROPSCH SYNTHESIS: CHARACTERIZATION OF INTERACTIONS BETWEEN REDUCTION PROMOTERS AND Co FOR Co/Al_2O_3-BASED GTL CATALYSTS

Gary Jacobs, Amitava Sarkar, Yaying Ji, Patricia M. Patterson, Tapan K. Das, Mingsheng Luo, and Burtron H. Davis
Center for Applied Energy Research, The University of Kentucky, 2540 Research Park Drive #203, Lexington, KY 40511

Introduction

Fischer-Tropsch synthesis (FTS) is normally carried out with either a cobalt or iron-based catalyst depending on the ratio of H_2/CO in the feed. As a step in gas-to-liquids (GTL) technology, cobalt catalysts are often preferred [1,2] due to the low intrinsic water-gas shift (WGS) activity of cobalt. While in many typical supported-metal catalysts, a low metal loading is preferable for obtaining a high surface area of available active metal, the same is not the case with cobalt alumina FTS catalysts, a commercial catalyst for slurry-based GTL operations. Commercial catalysts are, in fact, heavily loaded with cobalt, and companies have reported ratios up to 30 g Co to 100 g alumina [1,2]. This is an impressive number, considering that many supported metal reforming catalysts contain only 0.005-1% of highly dispersed metal. One reason for the high loadings is due to the strong interaction of small cobalt oxide species with the alumina support. Increasing the cobalt cluster size weakens the interaction, allowing a greater fraction of the active cobalt metal to reduce. Compare the hydrogen chemisorption / pulse reoxidation data in Table 1 for the 15% and 25%Co loadings for catalyst reduced at 350°C for 10 hours, which is a common reduction condition for Fischer-Tropsch synthesis catalysts. The 25%Co catalyst exhibits 42% reduction versus 30% for the 15%Co catalyst, but the average diameter is larger (11.8 nm versus 5.9 nm for the 15%Co loading). The reduction of cobalt oxides on alumina follows primarily a two step reduction process from Co_3O_4 to CoO, and from CoO to Co metal [3]. While the first reduction step is quite facile, occurring at ~350°C, it is the second step which depends strongly on the interaction with the support. It would be beneficial to develop active catalysts with lower cobalt loadings, and one way to accomplish this is to facilitate reduction of the smaller and more strongly interacting cobalt oxide species by promoting the catalyst with a reduction promoter, like Pt, Ru, or Re. As shown in Table 1, addition of a small amount of Pt to the low loading 15%Co catalyst doubles the extent of reduction while maintaining a small cluster size [3].

Table 1: Influence of loading and promoter addition to size and % reduction [3].

Catalyst	H_2 desorbed (μmoles per gram)	Uncorrected % Dispersion	Uncorrected diameter (nm)	% Reduction	Corrected % Dispersion	Corrected Diameter (nm)
$15\%Co/Al_2O_3$	66.9	5.3	19.6	30	17.5	5.89
$25\%Co/Al_2O_3$	77.7	3.7	28.2	42	8.7	11.8
$0.5\%Pt\text{-}15\%Co/Al_2O_3$	141	11.0	9.30	60	18.4	5.60

While these catalysts do exhibit impressive initial activity, unfortunately, they deactivate quite rapidly compared to the more heavily cobalt-loaded commercial catalysts. The smaller clusters appear to be more prone to sintering [4-7], and in water co-feeding studies [8-13], they have been found to be more sensitive than the more heavily loaded cobalt catalysts to support-induced reoxidation phenomena,

which likely involve cobalt-support complex formation [8,9,11-16]. These deactivation processes appear to be cluster size sensitive. Some researchers have chosen to explore the preparation of cobalt catalysts with much weaker support interactions (e.g., silica [17-19], carbon nanotubes [20]) to benefit from high reducibility. However, here we have taken a different course and opted to try to improve cobalt/alumina catalysts, as the support interaction appears to be important for the stabilization of a small cluster size. Furthermore, alumina benefits as a support for being very attrition resistant, a property that is key for slurry phase FT processes.

Therefore, in this work, the aim is to develop a better working cobalt/alumina catalyst with a low cobalt loading (~15%Co). The goal is to maintain the presence of a reduction promoter in the catalyst to assist in the reduction of the smaller, more highly interacting cobalt oxide species. Yet at the same time, the interest is to use pretreatments to essentially grow the cobalt cluster to a suitable size that is resistant to cluster size-related deactivation phenomena. Oxidation-reduction cycles have in the past proven fruitful for accelerating the aging (i.e., sintering) of metal particles, and this technique was chosen for ripening the cobalt clusters. One additional benefit of the method may be improved mixing between the active metal and the promoter [21].

In this investigation, 2%Ru-15%Co/Al_2O_3 was prepared by a wet impregnation technique. Oxidation-reduction cycles were performed on the material, and the impact on resulting cluster size, extent of reduction, degree of promoter interaction, and catalytic behavior were assessed.

Experimental

A large batch of 2%Ru-15%Co/Al_2O_3 catalyst was prepared by a wet impregnation method using cobalt nitrate and ruthenium nitrosyl nitrate as precursors. The cobalt was added first, with vacuum drying in a rotary evaporator, and the ruthium second. The catalyst was calcined in air flow at 350^{o}C for four hours. A batch of catalyst was removed (fresh calcined catalyst), and the remaining catalyst was reduced in H_2:Ar (1:2) mixture at 350^{o}C for 5 hours. The catalyst was cooled to room temperature in the H_2:Ar mixture, purged in argon, and then passivated using 1%O_2:He. A batch of catalyst was removed (RP#1 for reduced-passivated #1). The remaining catalyst was re-introduced to the reactor, and again, calcined, reduced for 5 hours, cooled, and passivated. Batch RP#2 was removed, and the process was carried out two more times to yield RP#3 and RP#4. However, for RP#3 and RP#4, the additional reduction cycles lasted 10 hours.

For TPR studies, the fresh catalyst, and calcined (air flow, 350^{o}C) catalysts of RP#1, RP#2, RP#3 and RP#4 were evaluated to study the impact of the pretreatments on catalyst reducibility. The profiles were recorded using a Zeton-Altamira AMI-200 unit which makes use of a TCD detector. The samples were first ramped to 350^{o}C in pure Ar to drive off any residual H_2O from the sample, prior to cooling to 50^{o}C to begin the TPR. The tests were performed using 10%H_2/Ar mixture referenced to Ar at a flow rate of 30 ccm. The samples were heated to 800^{o}C at a ramp rate of 10^{o}C per min.

Samples RP#1 - 4 were also evaluated by XANES and EXAFS spectroscopy at Brookhaven National Laboratory. Catalysts were re-reduced in the in-situ flow cell in flowing H_2 to 350^{o}C and held for 30 min, prior to cooling to liquid nitrogen temperatures in flowing H_2 for EXAFS analysis. Data were fitted using the WinXAS [22], Atoms [23], FEFF [24], and FEFFIT [24] programs. The k-window was typically chosen to be 3-15 A^{-1}.

The reduced/passivated catalysts were also examined by Transmission Electron Spectroscopy.

For reaction testing, 10g of the "fresh calcined catalyst" or "RP#3" was reduced for 10 hours in H_2 in an external fixed bed reactor prior to cooling in H_2 and transferring under Ar to the CSTR, where the catalyst was combined with 310 g of startup Polywax 3000. The catalyst was further pretreated with H_2 at 250°C for 24 hours. The initial conditions for the reactor were 280 psig, 220°C, with traps set at 200, 100, and 0°C, respectively. The feed gas was initially set to 80 slph with a composition of 66.66% H_2, 33.34% CO for a H_2:CO ratio of 2.0 and WHSV of 8.0. During the course of the run, the WHSV was adjusted to 5.0 and 3.0, the latter condition representing a point of CO conversion above 50%.

Results and Discussion

TPR profiles are reported in Figure 1. The arrows indicate starting from the freshly calcined catalyst and moving toward a greater number of oxidation-reduction cycles. It is clear that, relative to unpromoted 15%Co/Al_2O_3, which completely reduces only at ~800°C, there is a shift in the reduction temperatures of both steps (i.e., Co_3O_4 to CoO and CoO to Co) to much lower temperatures (~150-200°C shift) with addition of the Ru promoter. The oxidation-reduction cycles led to a shift to higher temperature for the 1st reduction step, but, more importantly, to a decrease in the required temperature for the 2nd step. To better understand the degree of catalyst reduction for both the Co and Ru components, XANES was utilized.

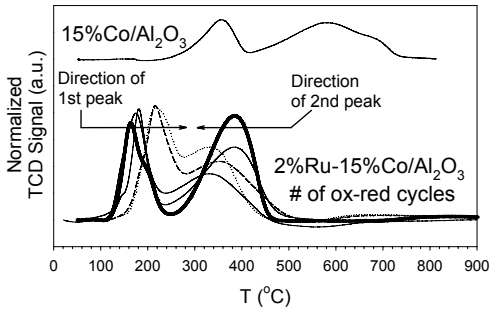

Figure 1: TPR profiles of 15%Co/Al_2O_3 and 2%Ru-15%Co/Al_2O_3 catalysts after a series of oxidation reduction cycles.

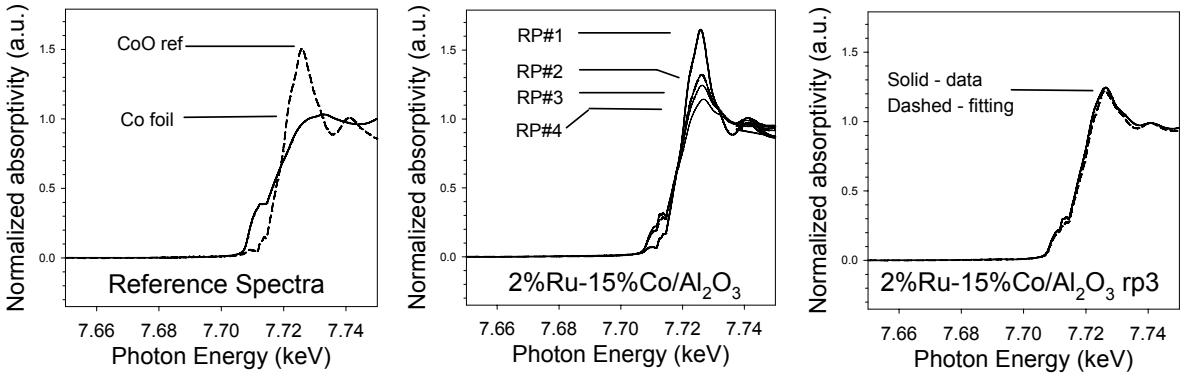

Figure 2: XANES profiles at the Co K-edge of (left) Co reference compounds; (center) 2%Ru-15%Co/Al_2O_3 catalysts after the oxidation-reduction cycle treatments; and (right) sample linear combination XANES fitting.

Figure 2 (left) displays the reference compounds for Co^0 and CoO, the two states present after the catalyst is reduced. Figure 2 (center) shows that little Co^0 was present after the first 5 hour reduction treatment. However, with additional oxidation-reduction cycles, the cobalt systematically becomes more reduced. The spectra were fitted by taking a linear combination of the Co^0 and CoO references and a sample fitting is provided in Figure 2 (right). The increasing extent of catalyst reduction is quantified in Table 2.

Table 2: Results of linear combination XANES fitting - Co component.

Catalyst	% CoO	% Co^0
2%Ru-15%Co/Al_2O_3 rp#1	95.0	5.0
2%Ru-15%Co/Al_2O_3 rp#2	58.6	41.4
2%Ru-15%Co/Al_2O_3 rp#3	47.2	52.8
2%Ru-15%Co/Al_2O_3 rp#4	35.9	64.1

Interestingly, the Ru promoter is in a completely reduced state in all cases. The promoting effect of Ru may be an electronic influence due to alloying, or more likely, by providing sites for the dissociation and spillover of H_2, which can aid in nucleating the formation of reduced sites on the cobalt oxide species. The XANES results are in agreement with the shifts observed by TPR.

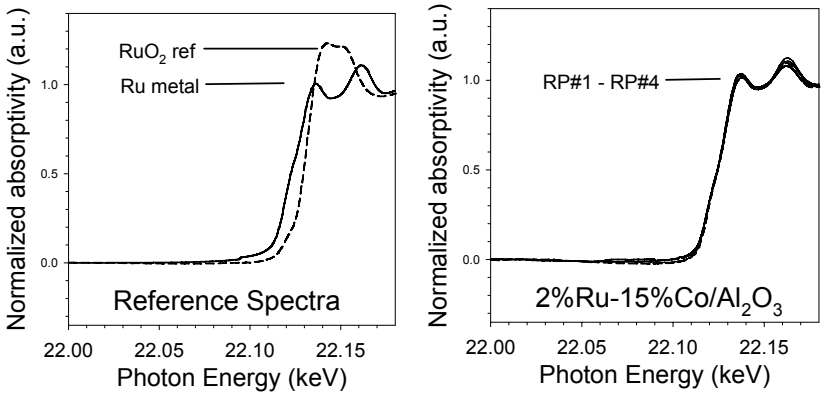

Figure 3: XANES profiles at the Ru K-edge of (left) reference compounds and (right) 2%Ru-15%Co/Al_2O_3 RP#1-RP#4 catalysts. The spectra virtually overlap.

EXAFS spectra of Co reference spectra are reported in Figure 4, while data for the 2%Ru-15%Co/ Al_2O_3 catalyst are reported for the RP#1-RP#4 treatments (i.e., increasing number of oxidation-reduction cycles). It is evident that after the first reduction of 5 hours, a large fraction of Co is CoO, as the peak for Co-Co in the CoO phase is greater than the peak for Co-Co coordination in the metal. With increasing oxidation-reduction cycles, however, the peak for Co-Co in the CoO decreases significantly, while the peak for Co-Co coordination in the metal increases, indicative of cluster growth.

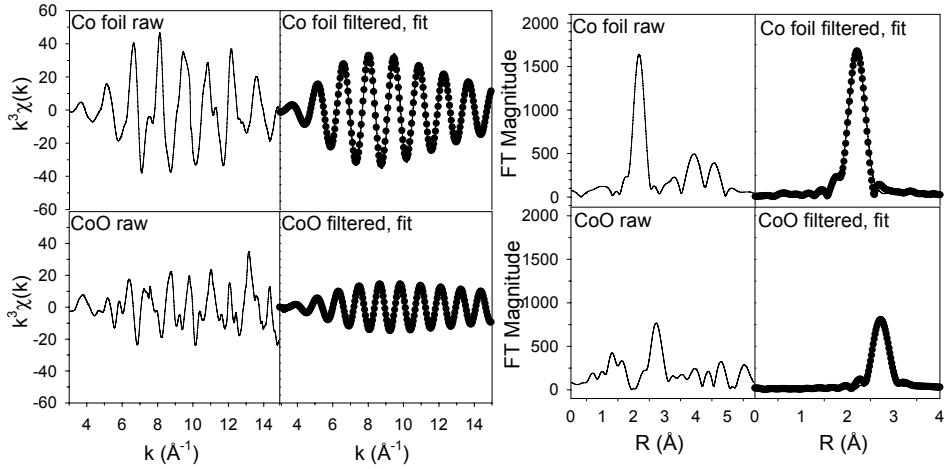

Figure 4: EXAFS results at the Co K-edge for the Co metal foil and CoO reference compounds, including filtering of the 1st Co-Co coordination shell and fitting.

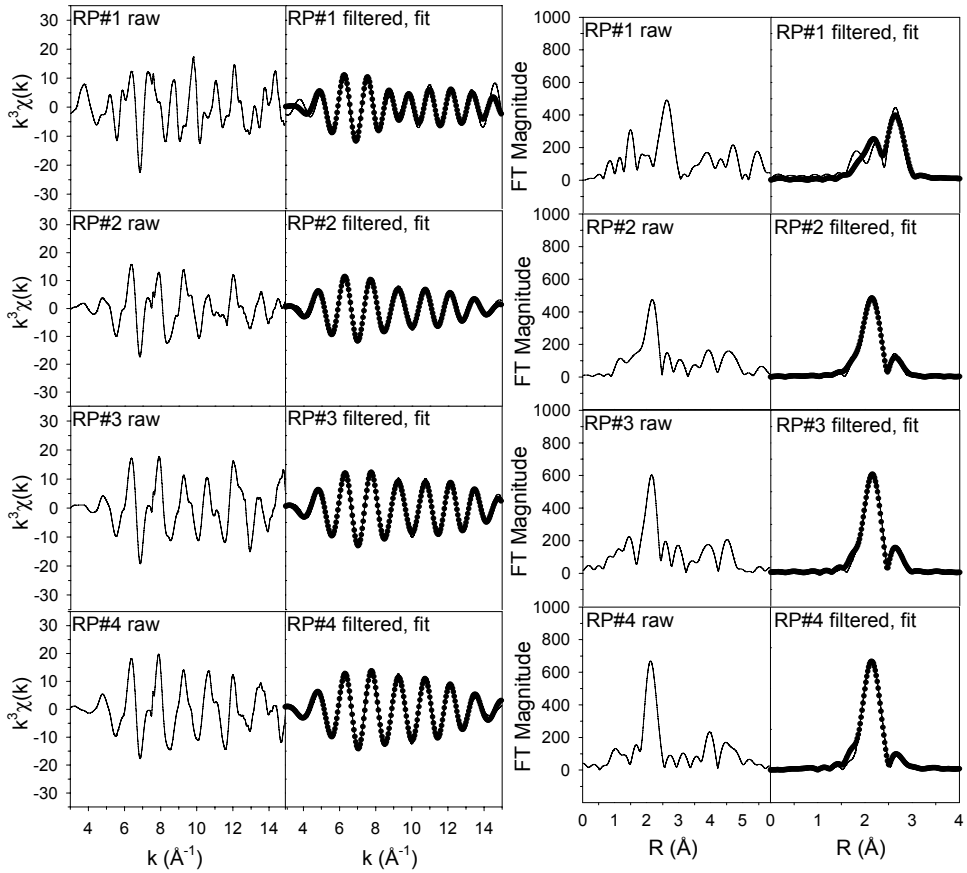

Figure 5: EXAFS results at the Co K-edge for the 2%Ru-15%Co/Al_2O_3 catalyst after reducing at 350^{o}C for 30 min of samples RP#1-RP#4. Note growth in Co-Co (metal) FT peak, indicative of a larger average Co cluster size.

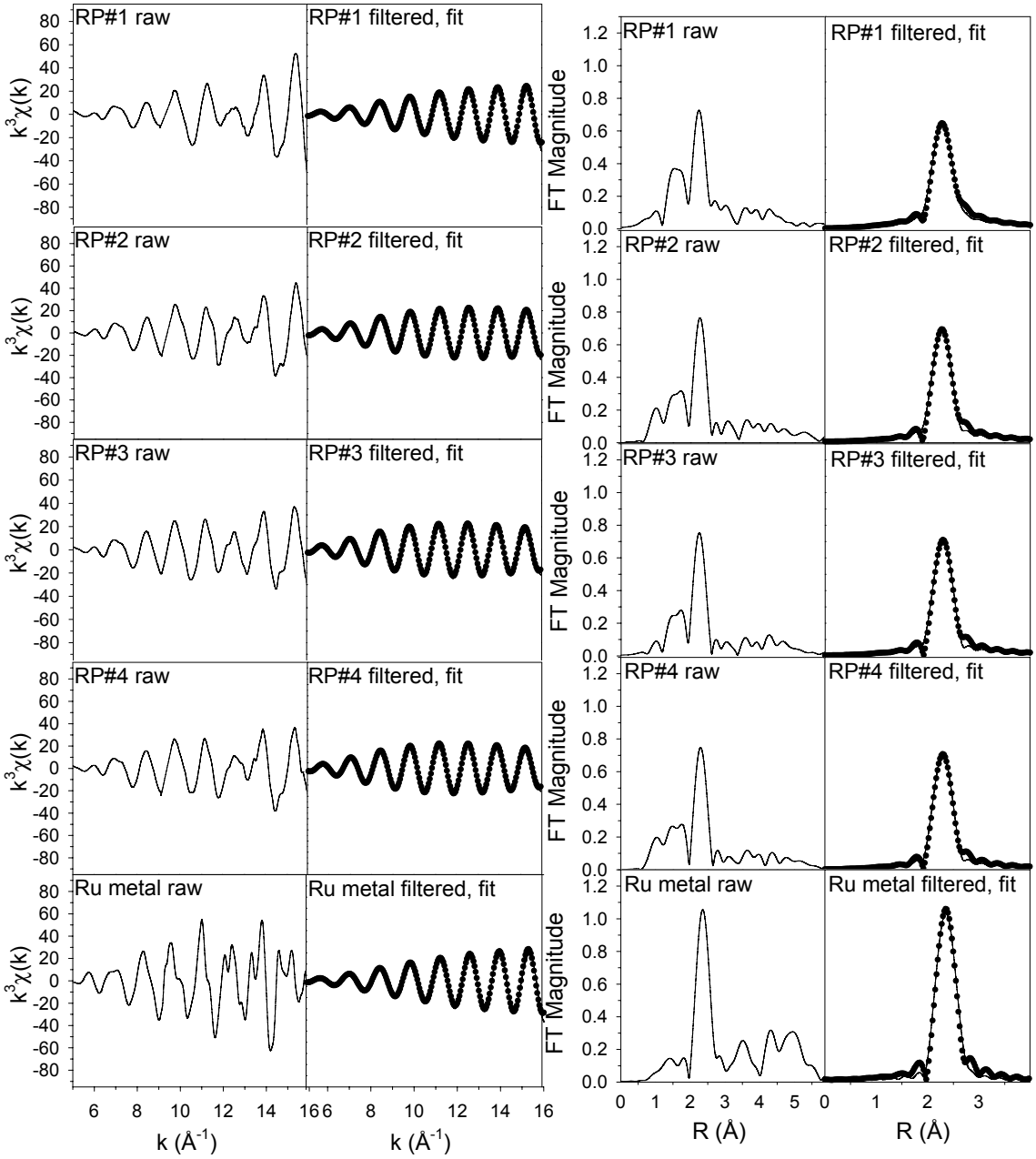

Figure 6: EXAFS results at the Ru K-edge for the 2%Ru-15%Co/Al_2O_3 catalyst after reducing at 350°C for 30 min of samples RP#1-RP#4.

The EXAFS spectra for Ru clearly indicate a Fourier transform magnitude peak for Ru-Ru coordination in the metal, which changes with the number of oxidation-reduction cycles. Interestingly, there are additional Fourier transform peaks at lower R. TEM results (to be presented) suggest Ru is located in the vicinity of Co.

Results of EXAFS fittings are provided in Table 3. For cobalt, both 1st shell Co-Co interactions (i.e., in the metal and in the CoO oxide) are included, while for Ru, only the 1st shell Ru-Ru interaction was fitted.

Table 3: EXAFS fitting parameters.

Co-Co first shell coordination in the Co^0 fraction

	n	Δn	S_0^2	ΔS_0^2	e_0	Δe_0	α	Δα	σ^2	$\Delta\sigma^2$	r
RP#1	4.68	3.12	**0.865**	-	-6.13	8.21	0.00566	0.0176	0.0101	0.00512	0.170
RP#2	5.82	0.66	**0.865**	-	-4.95	1.44	-0.000540	0.00250	0.00610	0.000665	0.00639
RP#3	6.00	0.64	**0.865**	-	-5.05	1.49	-0.00188	0.00234	0.00460	0.000630	0.00663
RP#4	6.40	0.80	**0.865**	-	-6.06	1.70	-0.00437	0.00263	0.00448	0.000675	0.00857
Co foil	**12**	-	0.865	0.084	8.32	1.32	-0.00323	0.00194	0.00332	0.000493	0.0113

note: set parameters in bold text

Co-Co first shell coordination in CoO fraction

	n	Δn	S_0^2	ΔS_0^2	e_0	Δe_0	α	Δα	σ^2	$\Delta\sigma^2$	r
RP#1	4.87	0.97	**0.865**	-	-5.61	2.31	-0.00975	0.00311	0.00354	0.000942	0.0145
RP#2	2.01	0.79	**0.865**	**-**	-5.56	4.42	-0.00655	0.00697	0.00584	0.00219	0.0152
RP#3	1.09	0.27	**0.865**	**-**	-7.89	2.96	-0.0142	0.00344	0.00179	0.00102	0.0189
RP#4	0.68	0.19	**0.865**	**-**	3.92	3.14	0.00693	0.00406	0.00202	0.00124	0.0335
CoO powder	7.01	0.71	**0.865**	-	3.00	1.15	0.00309	0.00146	0.001899	0.00044	0.0044

note: set parameters in bold text

Ru-Ru first shell coordination in the Ru^0 fraction. For Ru metal, Hanning window set to 1.96 – 2.75. For catalysts, the Hanning window was in the range 1.94 - 2.65.

	n	Δn	S_0^2	ΔS_0^2	e_0	Δe_0	α	Δα	σ^2	$\Delta\sigma^2$	r
RP#1	3.24	0.52	**0.889**	-	-9.10	2.73	-0.0324	0.00199	-0.000019	0.000469	0.00559
RP#2	5.33	0.92	**0.889**	-	-7.56	2.79	-0.0307	0.00227	0.00138	0.000545	0.00777
RP#3	6.25	1.11	**0.889**	-	-5.08	2.81	-0.0262	0.00239	0.00186	0.000578	0.00875
RP#4	6.61	0.92	**0.889**	-	-4.05	2.18	-0.0258	0.00189	0.00208	0.000460	0.00552
Ru^0	**12**	-	0.889	0.130	-1.43	2.23	-0.00707	0.00207	0.00261	0.000507	0.00756

note: set parameters in bold text

Again, the tabulated EXAFS results of the fittings indicate that the degree of Co-Co coordination in the metal increases, while the degree of Co-Co coordination in the oxide decreases. EXAFS and XANES results indicate that the average cobalt metal cluster size is increasing with the number of oxidation-reduction cycles, and that, in addition to the influence of the Ru promoter, with a resulting increase in the cluster size, the catalysts exhibit an enhanced extent of reduction. The Ru promoter also displays an increase in Ru-Ru coordination number as a function of the number of oxidation-reduction cycles, suggesting cluster growth. The impact of the effect of the oxidation-reduction cycles on the catalytic properties (i.e., activity and stability) will be discussed in the presentation.

References

(1) van Berge, P.J., Barradas, S., van de Loosdrecht, J., Visagie, J., "Advances in the cobalt catalyzed Fischer-Tropsch synthesis," Erdol Erdgas Kohle 117 (2001) 138-142.
(2) van Berge, P.J., van de Loosdrecht, J., Barradas, S., van der Kraan, A.M., "Oxidation of cobalt based Fischer-Tropsch catalysts as a deactivation mechanism," Catal. Today 58 (2000) 321-334.
(3) Jacobs, G., Das, T.K., Zhang, Y., Li, J., Racoillet, G., and Davis, B.H., "Fischer-Tropsch synthesis: support, loading, and promoter effects on the reducibility of cobalt catalysts," Appl. Catal. A 233 (2002) 281.
(4) Saib, A.M., Borgna, A., van de Loosdrecht, J., van Berge, P.J., and Niemantsverdriet, J.W., "XANES study of the susceptibility of nano-sized cobalt crystallites to oxidation during realistic Fischer–Tropsch synthesis," Appl. Catal. A 312 (2006) 12-19.
(5) Bertole, C.J., Mims, C.A., Kiss, G., "The effect of water on the cobalt-catalyzed Fischer-Tropsch synthesis," J. Catal. 210 (2002) 84-96.
(6) Jacobs, G., Patterson, P.M., Zhang, Y., Das, T.K., Li, J., Davis, B.H., "Fischer-Tropsch synthesis: deactivation of noble metal-promoted Co/Al_2O_3 catalysts," Appl. Catal. A 233 (2002) 215-226.
(7) Das, T.K, Jacobs, G., Patterson, P.M., Conner, W.A., Li, J., Davis, B.H., " Fischer-Tropsch synthesis: characterization and catalytic properties of rhenium promoted cobalt alumina catalysts," Fuel 82 (2003) 805-815.
(8) Schanke, D., Hilmen, A.M., Bergene, E., Kinnari, K., Rytter, E., Adnanes, E., Holmen, A., "Study of the deactivation mechanism of Al_2O_3-supported cobalt Fischer-Tropsch catalysts," Catal. Lett. 34 (1995) 269-284.
(9) Hilmen, A.M., Schanke, D., Hanssen, K., Holmen, A., "Study of the effect of water on alumina supported cobalt Fischer-Tropsch catalysts," Appl. Catal. A 186 (1999) 169-188.
(10) Li, J., Zhan, X., Zhang, Y., Jacobs, G., Das, T.K., Davis, B.H., "Fischer-Tropsch synthesis: effect of water on the deactivation of Pt promoted Co/Al_2O_3 catalysts," Appl. Catal. A 228 (2002) 203-212.
(11) Jacobs, G., Das, T.K., Patterson, P.M., Li, J., Sanchez, L., Davis, B.H., "Fischer-Tropsch synthesis: XAFS studies of the effect of water on a Pt-promoted Co/Al_2O_3 catalyst," Appl. Catal. A 247 (2003) 335-343.
(12) Jacobs, G., Patterson, P.M., Das, T.K., Luo, M., Davis, B.H., "Fischer-Tropsch synthesis: effect of water on Co/Al_2O_3 catalysts and XAFS characterization of reoxidation phenomena," Appl. Catal. A 270 (2004) 65-76.
(13) Storsaeter, S., Borg, O., Blekkan, E.A., Holmen, A., "Study of the effect of water on Fischer-Tropsch synthesis over supported cobalt catalysts," J. Catal. 231 (2005) 405-419.
(14) Zhang, Y., Wei, D., Hammache, S., Goodwin, Jr., J.G., "Effect of water vapor on the reduction on Ru-promoted Co/Al_2O_3," J. Catal. 188 (1999) 281-290.
(15) Jongsomjit, B., Panpranot, J., and Goodwin, Jr., J.G., "Co-support compound formation in alumina-supported cobalt catalysts," J. Catal. 204 (2001) 98-109.

(16) Sirijaruphan, A., Horvath, A., Goodwin, Jr., J.G., Oukaci, R., "Cobalt aluminate formation in alumina-supported sobalt catalysts: effects of cobalt reduction state and water vapor," Catal. Lett. 91 (2003) 89-94.
(17) Bartholomew, C.H., Zennaro, R., Huber, G.W. , "Kinetics of Fischer-Tropsch synthesis on titania- and silica-supported cobalt," 217th ACS National Meeting, Anaheim, Calif., March 21-25 (1999).
(18) Krishnamoorthy, S., Tu, M., Ojeda, M.P., Pinna, D., Iglesia, E., "An investigation of the effects of water on rate and selectivity for the Fischer-Tropsch synthesis on cobalt-based catalysts," J. Catal. 211 (2002) 422-433.
(19) Bezemer, G., Leendert, Bitter, J.H., Kuipers, H.P.C.E., Oosterbeek, H., Holewijn, J.E., Xu, X., Kapteijn, F., van Dillen, A.J.; de Jong, K.P., "Cobalt Particle Size Effects in the Fischer-Tropsch Reaction Studied with Carbon Nanofiber Supported Catalysts," J. Am. Chem. Soc. 128 (2006) 3956-3964.
(20) Dalai, A.K., Das, T.K., Chaudhari, K.V., Jacobs, G., Davis, B.H., "Fischer-Tropsch synthesis: water effects on Co supported on narrow and wide-pore silica," Appl. Catal. A 289 (2005) 135-142.
(21) Iglesia, E., "Review: Design, synthesis, and use of cobalt-based Fischer-Tropsch synthesis catalysts," Appl. Catal. A 161 (1997) 59-78.
(22) T. Ressler, WinXAS 97, Version 1.0, 1997.
(23) B. Ravel, "EXAFS analysis using FEFF and FEFFIT workshop," 27 June, 2001.
(24) M. Newville, B. Ravel, D. Haskel, E.A. Stern, Y. Yacoby, "Analysis of multiple-scattering XAFS data using theoretical standards," Physica B 208-209 (1995) 154-156.